Toxicology Reports 1 (2014) 74–84

Contents lists available at ScienceDirect

Toxicology Reports

journal homepage: www.elsevier.com/locate/toxrep

In vivo and *in vitro* toxicity of nanogold conjugated snake venom protein toxin GNP-NKCT1

Partha Pratim Saha [a], Tanmoy Bhowmik [a], Anjan Kumar Dasgupta [b], Antony Gomes [a,*]

[a] *Laboratory of Toxinology & Experimental Pharmacodynamics, Department of Physiology, University of Calcutta, 92 APC Road, Kolkata 700009, India*

[b] *Department of Biochemistry, University of Calcutta, 35 Ballygunge Circular Road, Kolkata 700019, India*

ARTICLE INFO

Article history:
Received 22 January 2014
Received in revised form 14 April 2014
Accepted 14 April 2014
Available online 2 May 2014

Keywords:
Snake venom
Naja kaouthia
NKCT1
Toxicity study
GNP conjugation
GNP-NKCT1

ABSTRACT

Research on nanoparticles has created interest among the biomedical scientists. Nanoparticle conjugation aims to target drug delivery, increase drug efficacy and imaging for better diagnosis. Toxicity profile of the nanoconjugated molecules has not been studied well. In this communication, the toxicity profile of snake venom cytotoxin (NKCT1), an antileukemic protein toxin, was evaluated after its conjugation with gold nanoparticle (GNP-NKCT1). Gold nanoparticle conjugation with NKCT1 was done with $NaBH_4$ reduction method. The conjugated product GNP-NKCT1 was found less toxic than NKCT1 on isolated rat lymphocyte, mice peritoneal macrophage, in culture, which was evident from the MTT/Trypan blue assay. Peritoneal mast cell degranulation was in the order of NKCT1 > GNP-NKCT1. The *in vitro* cardiotoxicity and neurotoxicity were increased in case of NKCT1 than GNP-NKCT1. On isolated kidney tissue, NKCT1 released significant amount of ALP and γ-GT than GNP-NKCT1. Gold nanoconjugation with NKCT1 also reduced the lethal activity in mice. *In vivo* acute/sub-chronic toxicity studies in mice showed significant increase in molecular markers due to NKCT1 treatment, which was reduced by gold nanoconjugation. Histopathology study showed decreased toxic effect of NKCT1 in kidney tissue after GNP conjugation. The present study confirmed that GNP conjugation significantly decreased the toxicity profile of NKCT1. Further studies are in progress to establish the molecular mechanism of GNP induced toxicity reduction.

1. Introduction

Venom and toxins from the faunal and floral community of this world hold promise as medicinal agents that have been mentioned in ancient literatures Ayurvada, Unani, homoeopathy. Calmette [1] first showed that snake (*Naja* sp.) venom possesses anticancer potential. Many reports are available on the therapeutic potential of venom and toxins against experimental pathophysiological conditions [2,3]. drCT-1, a protein toxin isolated from the snake *Daboia russelii* venom, NKCT1 purified from Indian monocellate cobra (*Naja kaouthia*) venom and NN-32 isolated from snake (*Naja naja*) venom, showed anti-cancer activity [3–5]. *N. kaouthia* venom showed antiarthritic potential in experimental animal model [2]. Crototoxin isolated from *Crotelus durisus terrificus* venom has anticancer activity against human and murine tumour cell line [6]. VRCTC-310 produced by the combination of two different purified snake venom proteins also possesses anticancer activity [7]. Cobra toxin, isolated from snake *Naja naja atra* venom,

* Corresponding author. Tel.: +91 33 23508386/6387/6396/1397x229; fax: +91 33 2351 9755/2241 3288.
E-mail addresses: agomescu@gmail.com, gomesantony@hotmail.com (A. Gomes).

http://dx.doi.org/10.1016/j.toxrep.2014.04.007

has antinociceptive activity in mice. It has been found that pre-treatment with cobra venom factor delayed the acute inflammation of chronic arthritis in rat model. It depleted rat complement protein C_3 and inhibited the inflammatory response in adjuvant induced arthritis [8]. One of the major drawbacks of these bioactive molecules is their toxicity, which does not allow them to proceed further in drug development process. In order to overcome the toxicity, several attempts have been made including liposome encapsulation, silica coating, nanoconjugation, *etc.* [9,10].

Nanotechnology tunes the physical and chemical properties of a substance at molecular level, uses materials and devices designed to interact with the body at subcellular/tissue specific level with an aim to have maximum therapeutic and minimum adverse effects [11]. Use of nanotechnology against cancer, cardiac, neurodegenerative and inflammatory disorders was already reported. Evidences in synthesis and functionalization of nanoparticles have brought attention in the field of biomedical applications including imaging, drug delivery, sensing of target molecules [12].

Application of nanotechnology in the field of toxinology has increased the efficacy of the bioactive toxin molecules [13]. Mellitin, from bee venom, is a potential candidate for anticancer therapy, having disadvantages like nonspecificity and unfavourable pharmacokinetics. Soman and co-workers conjugated mellitin in the outer lipid monolayer of perflurocarbon (PFC) nanoparticles. The nanocarrier allows selective deliverance of mellitin to multiple tumour targets without apparent sign of toxicity [14]. Bombesin peptide obtains from toad skin showed protective activity against prostate, breast, and small cell lung carcinoma in experimental studies. It was conjugated with gold nanoparticle (GNP), which increased its affinity towards gastrin releasing peptide (GRP) receptors, overexpressed on tumour cells. Bombesin–gold conjugation also showed reduced reticulo-endothelium system uptake by organs with concomitant increase in uptake at tumour targets, which reduced its toxic manifestation towards the cells, other than the tumour tissue [15].

Gomes et al. [2] showed that *N. kaouthia* venom (NKV) had antiarthritic potential in experimental animals. A protein toxin NKCT1 isolated from NKV possesses anticancer activity [3]. Although it offered beneficial effects against experimental pathophysiological conditions, toxicity of NKCT1 was also reported [16]. Recently Bhowmik et al. [9] conjugated the protein toxin NKCT1 with PEGylated gold nanoparticles by using $NaBH_4$ reduction technique, which increased the anticancer property of NKCT1. However, the toxicity of nanogold conjugated NKCT1 needs to be assessed for its safety evaluation. The present study was an effort to investigate the toxicity profile of GNP-NKCT1 molecule through *in vivo* and *in vitro* study.

2. Materials and methods

2.1. Chemicals

Chemicals and reagents used were of analytic grade. The following chemicals were used – acrylamide (SRL, India); ammonium persulphate (SRL, India); bisacrylamide (SRL, India); bromophenol blue (Merck, India); carboxymethyl cellulose (Sigma, USA); creatine kinase, brain and muscle isoenzyme (CK-MB) kit (Ecoline, Merck, India); coomassie brilliant blue (Sigma, USA); disodium hydrogen phosphate (SRL, India); drabkin solution (Cogent, India); Diastix-Reagent Strips (Merck, India); EDTA (SRL, India); eosin (Qualigen, India); folin ciocalteu reagent (SRL, India); glycine (SRL, India); $HAuCl_4$ (Sigma, USA); haematoxylin (Qualigen, India); histopaque (Sigma, USA); KCl (SRL, India); *Lactate dehydrogenase* (LDH) kit (Merck, India); mercaptoethanol (SRL, India); methylene blue (Merck, India); MTT (Sigma, USA); $NaBH_4$ (SRL, India); P-nitrophenyl phosphate (SRL, India); poly(ethylene)glycol (SRL, India); RPMI-1640 medium (GIBCO, USA); TRIS (SRL, India); SDS (Merck, India); *Serum glutamic oxaloacetic transaminase* (SGOT)/serum glutamic pyruvic transaminase (SGPT) kit (Merck, India); sodium dihydrogen phosphate (SRL, India); sodium lauryl sulphate (SRL, India); TEMED (Merck, India); and urea kit (Merck, India).

2.2. Purification of NKCT1

Lyophilized *N. kaouthia* venom was collected from Calcutta Snake Park, Kolkata, India. Venom concentration was expressed in terms of dry weight/protein equivalent [17]. NKCT1 was purified from NKV by ion exchange chromatography and HPLC as reported earlier [3]. The fraction was desalted and concentrated by Centricon (Millipore MWCO 3k). Homogeneity of NKCT1 was checked by SDS-polyacrylamide gel electrophoresis (PAGE) method [18].

2.3. Synthesis of GNP-NKCT1

The gold nanoparticles were prepared by sodium borohydrate reduction method [9] with modification. 200 μl $HAuCl_4$ (20 mM) and 10 μl PEG (10 mg ml^{-1}) were mixed with 800 μl of sterile phosphate buffer (10 mM, pH 7.2). Then 40 μl of $NaBH_4$ (100 mM) was added drop wise and stirred at 37 °C for 1 h. Just after mixing the $NaBH_4$, the colour of the reaction mixture was light violet and after several minutes, it changed to deep blue. After 1 h of stirring, mixture was kept in room temperature for 24 h. After that 832 μl protein toxin NKCT1 (1 mg ml^{-1}) was added into the reaction mixture and the suspension was kept at room 37 °C for conjugation.

2.4. Experimental animals

Swiss albino male mice (20 ± 2 g), Wister male albino rats (120 ± 10 g), male guinea pig (250 ± 10 g), and toad (80 ± 5 g) were obtained from the approved animal breeders of University of Calcutta, and kept in polypropylene cage at controlled temperature (25 ± 2 °C), with suitable light conditions (12 h light and dark cycle) and relative humidity (65 ± 5%). The animals were provided with pellet diet and water *ad libitum*. The animal experiments were conducted with prior approval from the Animal Ethics Committee, Dept. of Physiology, University of Calcutta (AEC Ref: 820/04/ac/CPC SEA. 2010, dated: 16.11.2011).

2.5. Collection and culture of rat blood lymphocyte

Blood was collected aseptically from the male albino Wister rats (120 ± 10 g) by cardiac puncture and transferred to heparinized vial. Lymphocytes were collected from the whole blood using Ficoll histopaque after proper dilution with sterile saline water. It was washed with PBS and cultured RPMI-1640 media. Cells were grown in a CO_2 Incubator at 37 °C with 5% CO_2 in humidified condition.

2.6. Collection and culture of mouse peritoneal macrophage

1 ml of 20% starch solution (w/v, ratio) was injected (i.p.) to male albino Swiss mice (20 ± 2 g). After 24 h, peritoneal fluid was aseptically collected and diluted with normal saline. Peritoneal macrophage was washed with PBS and cultured in RPMI-1640 at 37 °C with 5% CO_2 in humidified condition.

2.7. In vitro cellular toxicity study

2.7.1. Effect on rat lymphocyte and mouse peritoneal macrophage

Isolated rat blood lymphocytes (1×10^6) and mouse peritoneal macrophage (1×10^6) were seeded in 96 well plate and treated with NKCT1 (2 μg ml^{-1})/GNP-NKCT1 (2 μg ml^{-1}). MTT assay was done to confirm its cytotoxic effect [36]. After 18 h of incubation, 40 μl (5 mg ml^{-1}) of MTT solution was added and kept for another 4 h. The formazan granules formed by viable cells were dissolved in DMSO and the O.D. at 570 nm was measured with an ELISA reader (BioTek, ELx800). The cell growth inhibition studies were done by 0.2% trypan blue exclusion assay with direct count using haemocytometer counting chamber under light microscope (Olympus, Tokyo).

2.7.2. Effect on rat peritoneal mast cells

Peritoneum was collected from male albino Wistar rats. The omentum was placed in different watch glasses group 1: 0.5 ml normal saline (control), group 2: 0.5 ml normal saline and NKCT1 (2 μg ml^{-1}) and group 3: 0.5 ml normal saline and GNP-NKCT1 (2 μg ml^{-1}). It was incubated at 37 °C for 30 min. After incubation, the peritoneum from each group was put on clear glass slide in perfectly stretching condition and was fixed over flame. The slide was then treated with ethanol:chloroform:acetic acid (6:3:1) mixture for 15 min. After downgrading treatment with ethanol:water, the slides were stained with 0.1% aqueous toluidine blue. The excess stain was washed with distilled water and upgrading treatment with ethanol:water up to 100% ethanol. The slides were washed twice with xylene and mounted in DPX. The mast cell count was done under the light microscope and expressed in terms of % degranulation against control preparation [19].

2.8. In vitro organ/tissue toxicity study

2.8.1. Effect on isolated guinea pig heart and auricle

Isolated guinea pig heart was prepared after Langendorff [20] and perfused with oxygenated (95% O_2 + 5% CO_2) Tyrode's solution (NaCl 137 mM, KCl 2.7 mM, $CaCl_2 \cdot 2H_2O$ 2.6 mM, $MgCl_2 \cdot 6H2O$ 1.27 mM, $NaHCO_3$ 11.9 mM, NaH_2PO_4 0.4 mM and glucose 5.5 mM) containing double dextrose (2 g l^{-1}) and the temperature was maintained at 37 ± 1 °C. The preparation was treated with NKCT1 (2 μg ml^{-1})/GNP-NKCT1 (2 μg ml^{-1}) and contraction was recorded on a rotating smoked drum using a heart lever. Isolated guinea pig auricle was prepared after Burn [21] and suspended in oxygenated Tyrode's solution (29 ± 1 °C) in a 4 ml glass bath. The preparation was treated with NKCT1 (750 μg ml^{-1})/GNP-NKCT1 (750 μg ml^{-1}) and spontaneous contraction was recorded on a smoked drum by a lightly sprung lever.

2.8.2. Effect on isolated nerve muscle preparation

Isolated toad gastrocnemius sciatic (TGS) nerve was prepared and suspended in frog Ringer's solution (NaCl 154 mM, KCl 5.6 mM, $CaCl_2$ 2.2 mM, $NaHCO_3$ 6 mM, glucose 5.55 mM). Isolated rat phrenic nerve diaphragm (RPND) was prepared after [35] and suspended in a 6 ml glass bath containing oxygenated (95% O_2 + 5% CO_2) Tyrode's solution. Both the preparations were stimulated with a square wave electronic stimulator of 8 V, 0.5 ms duration, 0.2 Hz (Grass, USA, Model No. SD9). TGS preparations were treated with NKCT1 (20 μg ml^{-1}) and GNP-NKCT1 (20 μg ml^{-1}), RPND preparations were treated with NKCT1 (5 μg ml^{-1}) and GNP-NKCT1 (5 μg ml^{-1}) and contraction was recorded with Brodie's lever on a smoked kymograph paper.

2.8.3. Effect on isolated kidney tissue

Isolated rat kidney tissue (200 mg) was collected from a freshly killed male albino rat and suspended in oxygenated (95% O_2 + 5% CO_2) Kreb's Ringer solution (3 ml) in a glass tissue bath at (37 ± 1 °C). NKCT1 (2 μg ml^{-1})/GNP-NKCT1 (2 μg ml^{-1}) was added and incubated for 30 min. Incubation fluid was collected from control and treated tissue bath and immediately placed in ice (0 °C). The biochemical markers (ALP, γ-GT) were measured by biochemical kits (Merck, India). The kidney tissues were subjected to histopathology study (as stated earlier).

2.9. In vivo acute toxicity study

2.9.1. Determination of absolute lethal dose

Absolute lethal dose (LD_{100}) of NKCT1 and GNP-NKCT1 was determined in Swiss albino male mice. Different doses (1 mg kg^{-1}, 1.5 mg kg^{-1}, 2 mg kg^{-1}, 2.5 mg kg^{-1}, 2.75 mg kg^{-1}, 3 mg kg^{-1} and 3.5 mg kg^{-1}) of NKCT1 and GNP-NKCT1 were given to different animal groups (s.c.) and mortality was recorded up to 24 h of observation. The lowest dose that killed 100% of test animals was considered as the LD_{100}.

2.10. In vivo sub-chronic toxicity study

Sub-chronic toxicity study was done over a period of 15, 30 days in male albino Swiss mice (20 ± 2 g). The mice were divided into three groups: Group 1: sham control, group 2: NKCT1 treated (2 μg 100 g^{-1} day^{-1}, i.p.) and group 3: GNP-NKCT1 treated (2 μg 100 g^{-1} day^{-1}, i.p.) (n = 6). All the animals in groups 2 and 3 were treated for 15 and 30

days. Mortality, body weight, food and water intake, faecal consistency of all the animals were monitored at 5 days interval. Urine was collected from all groups of mice on day 30 and a qualitative analysis of urine parameters was done by Diastix reagent strips (Merck, India) and strip photograph was recorded (Nikon D90, Nikon 105 mm f/2.8 VR macro lens).

2.10.1. Haematology and serum biochemical parameters

Blood was collected from the control/treated animals on day 15, and day 30 by cardiac puncture and stored in heparin vials. Total WBC, RBC count and haemoglobin measurement were done. Serum was separated from the blood by centrifugation at 5000 rpm × 15 min. Serum biochemical parameters (SGOT, SGPT, urea, creatinine, CK-MB, LDH) were estimated by using biochemical kits (Merck, India) and UV–vis spectrophotometer (Analab UV-180) in the kinetic mode as per the instruction manuals.

2.10.2. Histopathology study

Kidney tissues of different groups of mice were collected on day 30 and dehydrated in graded alcohol (50%, 70%, 80%, 90% and 100%), cleared in xylene and embedded in paraffin. Sections (5 μm) were cut with rotary microtome (Weswox Optic, India), stained with haematoxylin–eosin, and observed under bright field microscope (Motic BA 450, Germany). Photographs were captured with Motic software (Motic Image Plus 2.0 software) to observe microscopic changes in the tissues.

2.11. Statistical analysis

Data were expressed as mean ± SEM ($n = 6$). The repeated measure analysis of variance (ANOVA) was used to determine the significant differences between groups. $P < 0.05$ was considered to be statistically significant.

3. Result

3.1. Purification of NKCT1

NKCT1 from NKV was purified as stated by Debnath et al. [3]. NKV was applied on CM-Cellulose column equilibrate with phosphate buffer (pH 7.2) and protein fractions were eluted with NaCl gradient and further purified over HPLC. Homogeneity of NKCT1 was checked by SDS-PAGE and SDS-molecular weight of the protein was found to be 6.76 kDa.

3.2. Nanogold conjugation and characterization of GNP-NKCT1

Preparation of GNP-NKCT1 was done with sodium borohydrate reduction method by using NKCT1, GNP, PEG, resulting in a light purple colour colloidal solution, stable at room temperature (25 ± 2 °C) and pH 7.2. Hydrodynamic size of GNP-NKCT1 determined by DLS was 68–122 nm with an average of 92 nm. Transmission electron microscope image confirmed the actual size of GNP as 5–25 nm, where gold nanoparticles were arranged within the protein (NKCT1) core [9].

3.3. In vitro cellular toxicity study

3.3.1. Effect on rat blood lymphocyte

MTT assay showed 28 ± 3.1% and 8 ± 2.6% inhibition of lymphocyte cell growth by NKCT1 (2 μg ml^{-1}) and GNP-NKCT1 (2 μg ml^{-1}) as compared with untreated control (Fig. 1A). Trypan blue exclusion assay revealed that there were 32 ± 1.2% and 11 ± 1.7% decrease in lymphocyte count by NKCT1 (2 μg ml^{-1}) and GNP-NKCT1 (2 μg ml^{-1}) treatment as compared to untreated control.

3.3.2. Effect on mouse peritoneal macrophage

MTT assay showed 38 ± 4.1% and 12 ± 1.5% inhibition of cell growth by NKCT1 (2 μg ml^{-1}) and GNP-NKCT1 (2 μg ml^{-1}) respectively as compared with untreated control (Fig. 1B). Trypan blue exclusion assay showed 34 ± 3.2% and 11 ± 2% decrease in rat peritoneal macrophage count by NKCT1 (2 μg ml^{-1}) and GNP-NKCT1 (2 μg ml^{-1}) treatment respectively as compared with untreated control.

3.3.3. Effect on rat peritoneal mast cell

NKCT1 (2 μg ml^{-1}) and GNP-NKCT1 (2 μg ml^{-1}) showed 30 ± 5% and 11 ± 2% degranulation of rat peritoneal mast cells respectively as compared with untreated control. However, standard drug (Tramazac) showed 85 ± 6% degranulation of mast cells, with respect to untreated control.

3.4. In vitro tissue toxicity study

3.4.1. Effect on isolated guinea pig heart

NKCT1 (2 μg ml^{-1}) decreased the amplitude of the contraction and heart rate leading to 100% irreversible heart blockade within 40 ± 5 min, whereas GNP-NKCT1 (2 μg ml^{-1}) treatment showed 100% irreversible heart blockade within 180 ± 10 min, which was 4.5-fold higher than that of NKCT1 (Fig. 2A and B).

3.4.2. Effect on isolated guinea pig auricle

NKCT1 (750 ng ml^{-1}) decreased the amplitude of the contraction leading to 50% blockade of isolated guinea pig auricle within 60 ± 3 min. GNP-NKCT1 (750 ng ml^{-1}) treatment showed 50% blockade within 180 ± 10 min, which was 3-fold higher than that of NKCT1 (Fig. 2C and D).

3.4.3. Effect on isolated RPND preparation

NKCT1 (5 μg ml^{-1}) decreased the amplitude of contraction induced by electrical stimulation leading to 50% neuromuscular blockade within 30 ± 2 min. GNP-NKCT1 (5 μg ml^{-1}) treatment showed 50% neuromuscular blockade within 180 ± 15 min, which was 6-fold higher than that of NKCT1 (Fig. 3A and B).

3.4.4. Effect on isolated TGS preparation

NKCT1 (20 μg ml^{-1}) decreased the amplitude of the contraction induced by electrical stimulation leading to

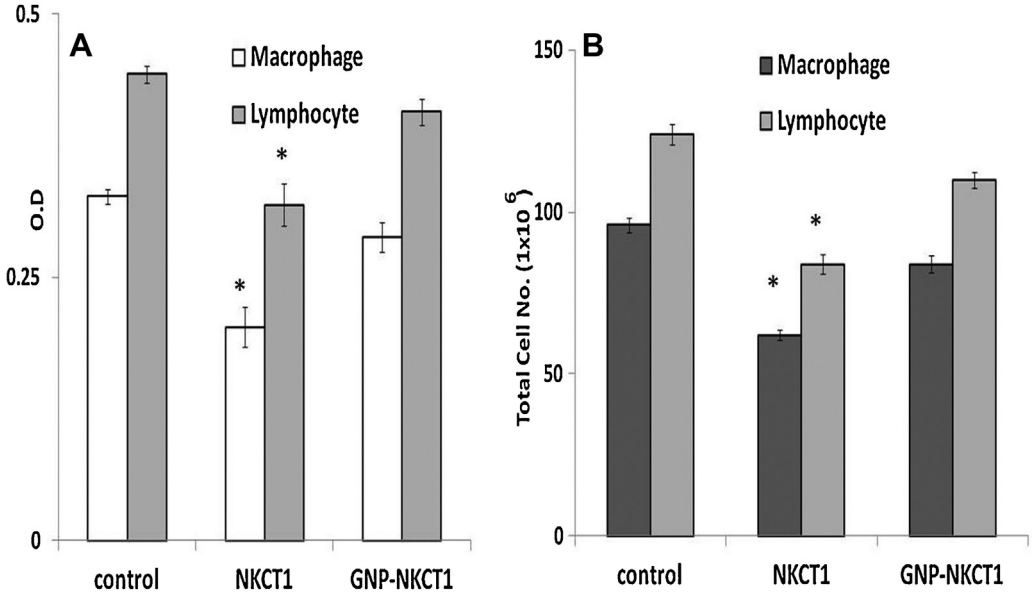

Fig. 1. Effect of NKCT1 and GNP-NKCT1 on normal rat lymphocyte, mouse peritoneal macrophage cells. Cell count by (A) MTT assay and (B) by trypan blue exclusion assays. Each value represents quadruplicate samples of mean ± SEM. *$P < 0.05$ as compared to control.

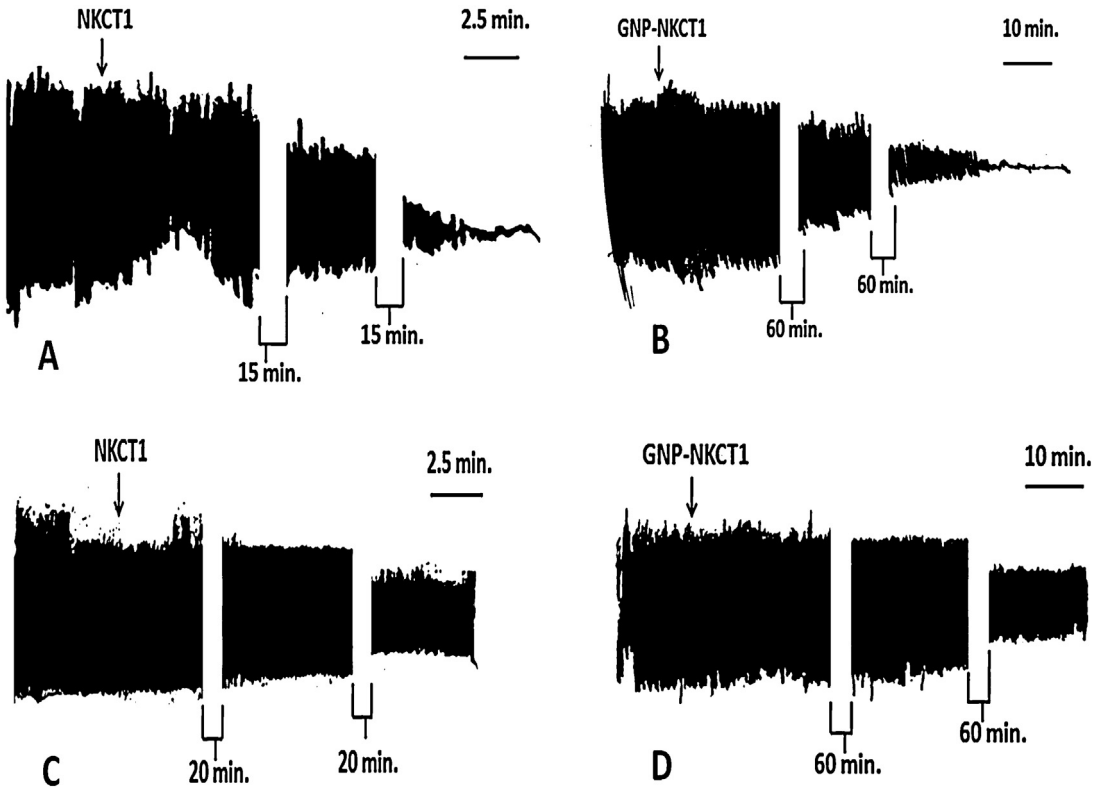

Fig. 2. Effect of NKCT1 and GNP-NKCT1 on isolated guinea pig. (A and B) heart, (C and D) auricle, (E and F) rat phrenic nerve diaphragm, and (G and H) toad gastrocnemius sciatic nerve. Time scale in minute.

50% neuromuscular blockade within 9 ± 2 min. GNP-NKCT1 (20 μg ml^{-1}) treatment showed 50% neuromuscular blockade within 180 ± 15 min, which was 20-fold higher than that of NKCT1 (Fig. 3C and D).

3.4.5. Effect on isolated rat kidney tissue

NKCT1 (2 μg ml^{-1}) significantly increased ALP (224.07 ± 18.9 U/L), released from kidney tissue, in respect to untreated control tissue (32 ± 2.9 U/L). However

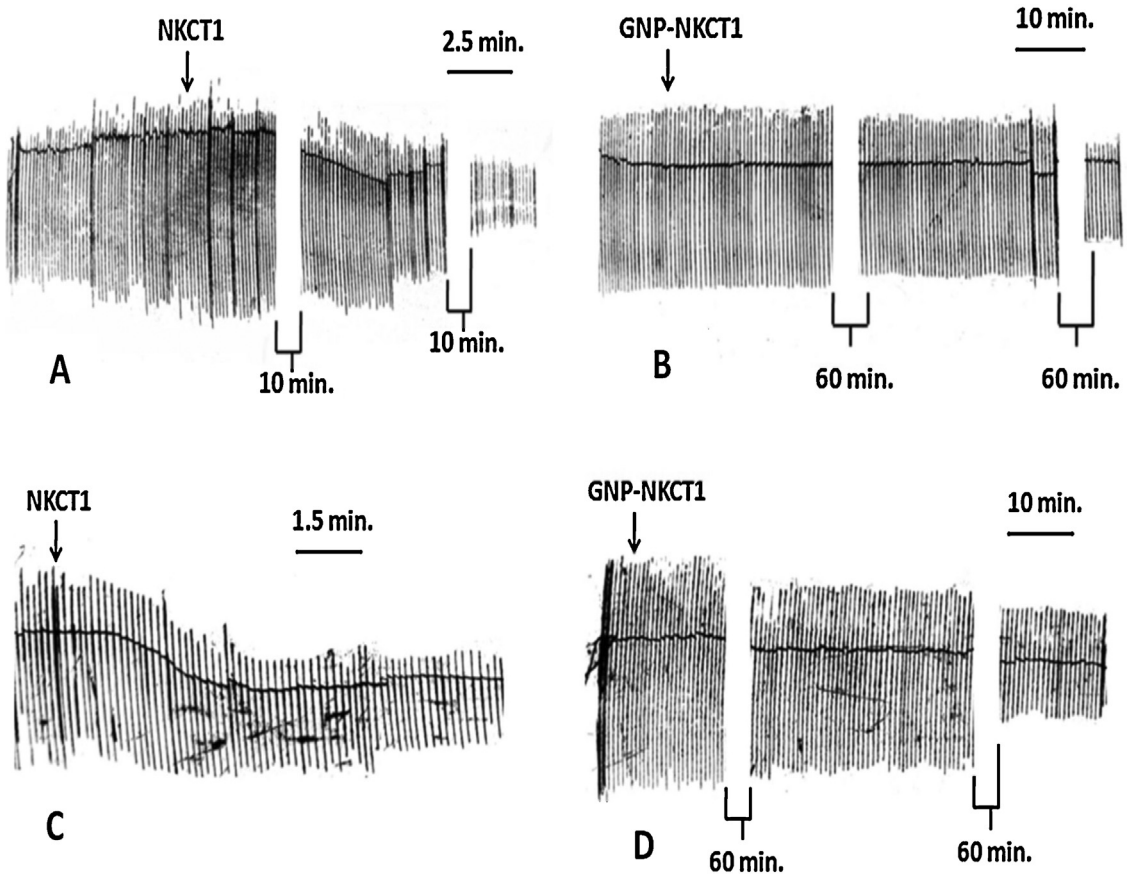

Fig. 3. Effect of NKCT1 and GNP-NKCT1 on isolated rat phrenic nerve diaphragm (A and B) and toad gastrocnemius sciatic nerve (C and D). Time scale in minute.

GNP-NKCT1 ($2\,\mu g\,ml^{-1}$) showed no significant increase in ALP (39.93 ± 6.15 U/L), released from kidney tissue, in respect to untreated control tissue. NKCT1 and GNP-NKCT1 treatment significantly increased γ-GT (73.24 ± 5.6 U/L and 43.26 ± 2.34 U/L), released from kidney tissue, in respect to untreated control tissue (26.34 ± 2.9 U/L). Histopathology study showed significant necrotic effect of NKCT1 on kidney tissue, which was not observed in case of GNP-NKCT1 treated kidney tissue (Fig. 5).

3.5. *In vivo acute toxicity study*

The absolute lethal dose of GNP-NKCT1 was found to be $3\,mg\,kg^{-1}$ (s.c.) in Swiss male albino mice, which was about 2-fold than that of NKCT1 ($1.5\,mg\,kg^{-1}$).

3.6. *In vivo sub-chronic toxicity study*

3.6.1. *Effect on body weight, food and water intake, faecal consistency, urine parameters*

No mortality was recorded up to 30 days in all the groups of mice. NKCT1 ($2\,\mu g\,100\,g^{-1}\,day^{-1}$, i.p.) treatment showed $22.2 \pm 1.9\%$ significant decreases in body weight in group 2 mice as compared with sham control group 1 mice. However GNP-NKCT1 ($2\,\mu g\,100\,g^{-1}\,day^{-1}$, i.p.) treated group 3 animals showed slow body weight gain, but no significant loss of body weight as compared with sham control group 1 mice (Fig. 4). NKCT1 treatment significantly reduced the food and water intake of

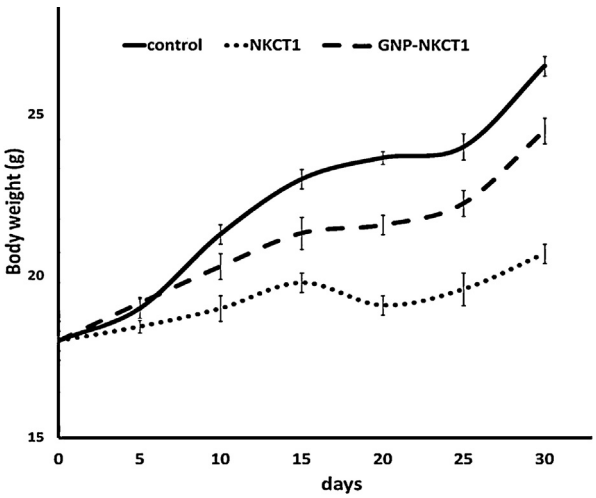

Fig. 4. Effect of NKCT1 and GNP-NKCT1 on body weight gain of different mice groups.

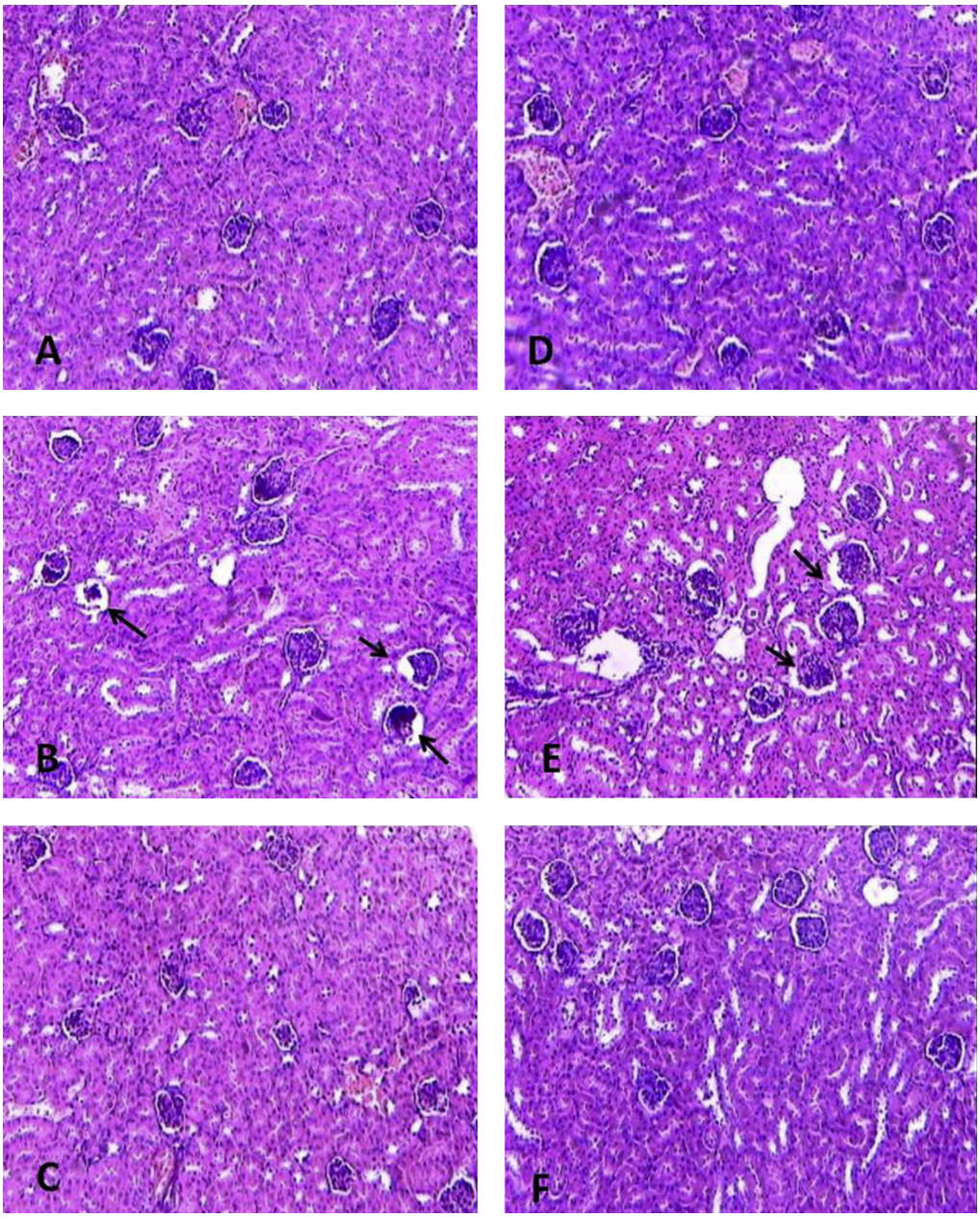

Fig. 5. Effect of GNP-NKCT1 and NKCT1 on kidney tissue, *in vivo* and *in vitro* study. Tissue stained with haematoxylin and eosin. Original magnifications 10×. (A–C) *In vivo* study with mice kidney tissue, where (A) denotes control tissue; (B) denotes NKCT1 treated tissue; (C) denotes GNP-NKCT1 treated tissue. (D–F) *In vitro* study with isolated rat kidney tissue, where (D) denotes control tissue; (E) denotes NKCT1 treated tissue; (F) denotes GNP-NKCT1 treated tissue. Arrows (↑) indicated the increased glomerular space and necrotic effect of NKCT1.

the group 2 mice after day 5 in respect to control group 1 and GNP-NKCT1 treated group 3 mice. Semisolid faecal pellets were observed by NKCT1 treated group 2 mice after day 9, whereas GNP-NKCT1 treated group 3 mice and sham control group 1 mice showed solid faecal pellets.

Urine strip test on day 30 revealed no changes in urinary glucose, bilirubin, ketone, specific gravity, blood, pH, urobilinogen in NKCT1 as well as GNP-NKCT1 treated groups 2 and 3 mice. However, urine of the NKCT1 treated group 2 mice showed high level of protein (+++) as compared with GNP-NKCT1 treated group 3 mice urine protein (+).

3.6.2. *Effect on haematological parameters*

On day 15, there were no significant changes in total RBC, WBC and haemoglobin level in NKCT1 and GNP-NKCT1 treated groups of mice. On day 30, there was a significant increase in WBC count that was observed in NKCT1 ($79.2 \pm 2.7\%$) and GNP-NKCT1 ($32.4 \pm 1.6\%$) treated

groups 2 and 3 mice in respect to sham control group 1 mice (Table 1).

3.6.3. Effect on serum biochemical parameters

On day 15, there was a significant increase in serum SGPT, urea, creatinine, CK-MB and LDH levels (40.7 ± 2.94%, 62.14 ± 2.36, 62.36 ± 1.31%, 80.94 ± 1.43 and 21.3 ± 1.7% respectively) due to NKCT1 treatment in group 2 mice as compared with sham control group 1 mice. However no significant change in serum SGPT, urea, creatinine, CK-MB and LDH was observed after GNP-NKCT1 treatment in group 3 mice as compared with sham control group 1 mice (Table 1).

On day 30, serum SGPT, urea, creatinine, CK-MB and LDH levels showed (18.12 ± 1.29%, 127.82 ± 2.14%, 102.5 ± 4.1%, 46.1 ± 1.39% and 49.27 ± 2.37%) significant increase after NKCT1 treatment in group 2 mice as compared with sham control group 1 mice. Serum urea, creatinine, and LDH levels (23.5 ± 1.39%, 20.21 ± 1.7%, and 14.7 ± 1.37%) were also significantly increased after GNP-NKCT1 treatment in group 3 mice in compared with sham control group 1 mice. The degree of increase was NKCT1 > GNP-NKCT1 (Table 1).

3.6.4. Effect on kidney histology

After 30 days, NKCT1 treated kidney tissue showed partial tubular and glomerular necrosis and increased capsular space. No such detrimental changes in kidney tissue of group 3 mice were observed after GNP-NKCT1 treatment (Fig. 5).

4. Discussion

Biomedical research using natural resources has identified animal venoms and toxins with great potential against various pathophysiological conditions. A major drawback of these bioactive toxin molecules is their toxicity, which limits their application in drug development process. Several attempts have been made to reduce the toxicity of these molecules, nanoconjugation being one of them. Nanoconjugation of therapeutically active toxin molecules will not only provide a mechanism for increasing their efficacy but also decreases toxicity. For instance, it was reported that mellitin from bee venom and bombesin from toad skin were conjugated to PFC and gold nanoparticles respectively which increased their selective delivery and cellular uptake in cancer cells, which limit their nonspecific off target toxicity [14,15]. Methotrexate (MTX) is clinically used as anti-arthritic and an anti-folate agent that is often associated with toxicity [22]. Gomes et al. [23] showed that nanogold conjugation with MTX (MTX-GNP) increased its anti-arthritic potential.

In vitro cellular toxicity studies showed that GNP-NKCT1 possesses about 3-fold less toxic effect on rat blood lymphocytes than that of NKCT1, as observed by MTT and trypan blue exclusion assay. Macrophages are the white blood cells produced by the division of monocytes, phagocytic in nature and acting in both non-specific (innate immunity) and specific defence mechanism (adaptive immunity). Trypan blue exclusion and MTT assay showed that NKCT1 (2 μg ml^{-1}) killed 40–46% peritoneal macrophage cell population after 24 h incubation, whereas

Table 1
Serum biochemical and haematological parameters after 15 and 30 days treatment.

Animal groups		Serum biochemical parameters						Haematological parameters		
		Creatinine (mg dl^{-1})	Urea (mg dl^{-1})	CK-MB (U L^{-1})	LDH (U L^{-1})	SGOT (U L^{-1})	SGPT (U L^{-1})	Total WBC (×1 mm^3)	Total RBC (million mm^3)	Hb (%)
15 days	Group 1	0.74 ± 0.03	27.3 ± 1.2	10.5 ± 0.4	163.23 ± 2.9	61.01 ± 2.2	22 ± 1.2	11.5 ± 0.7	9.4 ± 0.4	17.9 ± 1.2
	Group 2	1.23 ± 0.15*	44.4 ± 3.7*	19.02 ± 1.1*	206.9 ± 24.3*	66.63 ± 4.6	27.6 ± 1.5*	11.2 ± 0.3	9.5 ± 0.5	18.3 ± 0.8
	Group 3	0.78 ± 0.05	30.36 ± 2.18	11.9 ± 0.7	186.4 ± 11.1	51.83 ± 1.9	24.6 ± 2.1	10.7 ± 0.4	9.7 ± 0.4	18.1 ± 1.3
30 days	Group 1	0.78 ± 0.05	27.9 ± 0.9	10.4 ± 0.3	150.9 ± 3.7	58.8 ± 1.8	21.36 ± 0.8	10.4 ± 0.4	9.2 ± 0.8	18.5 ± 0.9
	Group 2	1.59 ± 0.17*	63.38 ± 2.8*	19.18 ± 0.9*	225 ± 26.3*	64.53 ± 2.7	26.2 ± 0.8*	18.4 ± 0.4*	8.8 ± 0.9	18.2 ± 1.3
	Group 3	0.94 ± 0.09*	34.47 ± 1.6*	10.6 ± 0.4	176.9 ± 9.4*	59.8 ± 1.8	21.83 ± 1	13.9 ± 0.2*	9.01 ± 0.8	18.9 ± 0.6

Data represent the mean ± SEM ($n = 6$).
* $P < 0.05$ considered as significant level, when compared to sham control group (group 1: sham control, group 2: NKCT1 treated mice, group 3: GNP-NKCT1 treated mice).

GNP-NKCT1 showed only 11–12% macrophage cell killing property. These data indicated that the adverse toxicity of NKCT1 on macrophage cell was significantly reduced (about 3-fold) after GNP conjugation. It was very likely with that PEGylgted gold nanoparticles conjugation with a snake venom protein toxin NKCT1 reduced its toxicity on human lymphocytes [9].

Mast cells mediate inflammatory responses such as hypersensitivity and allergic reactions. It stores a number of chemical mediators including histamine, interlukins, proteoglycans and various enzymes. Upon stimulation, mast cells release the chemical mediators that produce local allergic and inflammatory responses. Degranulation of mast cell is a common effect of toxin molecules. Toxin SA-HT isolated from butter fish venom [24], a basic PLA2 isolated from *Trimeresurus mucrosquamata* snake venom [25], produced oedema and increased capillary permeability by mast cell degranulation. In the present study, it was found the NKCT1 ($2\ \mu g\ ml^{-1}$) showed 30% degranulation of rat peritoneal mast cells, which was significantly reduced (3-folds) in the case of GNP-NKCT1 treatment. Thus GNP conjugation reduced the mast cell degranulation property as well as the pro-inflammatory effect of the NKCT1.

Cardiotoxicity is very common with snake venom toxins (NKCT1 and NN-32). *In vitro* cardiotoxicity on isolated heart and auricle preparation revealed that GNP-NKCT1 increased the blockage time of heart and auricle (4.5- and 3-folds respectively) than that of NKCT1. Protection against NKCT1 induced cardiotoxicity was further supported by serum levels of heart injury markers (CK-MB, LDH) in *in vitro* model. CK-MB helps to reserve energy through creatine phosphate and produce ATP as per requirement of the body. During the acute myocardial infarction, serum CK-MB level increased due to the release of intracellular CK-MB [26]. Lactate Dehydrogenase catalyzes the conversion of pyruvate to lactate. Patient with acute myocardial infarction, serum LDH level exceeds the normal range and reaches a peak elevation of two to three folds in 3–5 days [27]. Serum CK-MB and LDH level were increased due to NKCT1 treatment after 15 and 30 days in respect to sham control. This was likely due to myocardial damage induced by NKCT1. Animals exposed to GNP-NKCT1 showed no significant changes in serum CK-MB level after 15 days and 30 days treatment. No significant change in serum LDH level was observed after 15 days treatment with GNP-NKCT1. However after 30 days, animals exposed to GNP-NKCT1 showed a significant increase in serum LDH level ($17.1 \pm 1.6\%$), in respect to sham control mice. But increased serum LDH level in group 3 mice, after 30 days exposure to GNP-NKCT1, was significantly ($22 \pm 1.7\%$) low in respect to NKCT1 treated group 2 mice. The above findings indicated that GNP conjugation significantly reduces the cardiotoxicity of NKCT1.

Nephrotoxicity is one of the major characteristics of the snake venom molecules. Among the several nephrotoxicity markers, γ-glutamyl transpeptidase (γ-GT), a glycoprotein, attached to the external surface of various cell types. In the kidney, the primary site of γ-GT activity is the outer surface of the microvillus membrane (brush border) in the proximal tubular cells [28]. High enzyme activity of alkaline phosphates (ALP) was also found in the cells of proximal convoluted tubules [29]. γ-GT and ALP were considered as biomarkers for detecting renal tubular injury. The increased activity of these biomarkers, detected in urine and serum shortly after tubular injury, indicated their release from proximal tubular cells and suggested to predict acute renal failure. In the present study, we have observed that NKCT1 increased the release of APL and γ-GT from isolated rat kidney tissue. It is likely that NKCT1 acted on the PT cells and increased the release of ALP and γ-GT. GNP-NKCT1 treatment decreased the release of ALP ($82.2 \pm 2\%$) and γ-GT ($40.93 \pm 1.3\%$), as compared with NKCT1 treatment, indicated that GNP conjugation significantly reduced the nephrotoxic property of NKCT1. NKCT1 treatment significantly increased the serum urea, creatinine level. In case of GNP-NKCT1 treated mice there was no sign of increase in serum creatinine and urea level till day 15. However significant increase ($19.3 \pm 2.1\%$ and $23 \pm 1.8\%$) of serum creatinine and urea level in group 3 mice, in respect to sham control mice, was observed after 30 days treatment with GNP-NKCT1. The data provided in Table 1 clearly showed that increased serum creatinine and urea level in animals exposed to GNP-NKCT1 and NKCT1 after 30 days, were in the order of NKCT1 > GNP-NKCT1. That indicated the reduced nephrotoxic effect of NKCT1 after its GNP conjugation.

Toxicity of NKCT1 was reduced due to nanogold conjugation which was observed in *in vitro* cellular and organ toxicity as well as in *in vivo* LD_{100} and sub-chronic toxicity studies. The reduced toxicity of GNP-NKCT1 may be due to its less bioavailablity, because body recognizes hydrophobic GNP as foreign particle and the reticulo-endothelial system eliminates these from the blood stream and takes them up in the liver or the spleen or internalized by macrophages [30]. In the present investigation, GNP was coated with PEG during the preparation of GNP-NKCT1, which shifted the overall particle charge to the positive site by surface modification, thus blocking the electrostatic and hydrophobic interactions, which helped to prevent the internalization of GNP-NKCT1 by phagocytosis through the binding of opsonin proteins to particle surfaces. As a result it increased the bioiavailability of GNP-NKCT1 and also prevented agglomeration in *in vivo* system.

NKCT1 is a 6.76 kDa protein with single polypeptide chain having 60 amino acid residues. The amino acid sequence of the NKCT1 is "LKCNKLVPLF YKTCPAGKNL CYKMFMVSNK TVPVKRGCID VCPKNSLVLK YVCCNTDRCN". It possesses 4 intra molecular disulfide bonds (Uniport, entry name CX1_NAJKA, accession P0CH80). It has structural and functional similarity of 3 finger toxins isolated from cobra venom. 3FTXs consist of one polypeptide chain, their spatial structure being characterized by a hydrophobic core stabilized by four disulfide bridges, which confine three polypeptide loops (fingers). In cobra venom 3FTXs are represented mainly by α-neurotoxins and cytotoxins. 3FTXs neurotoxins use a number of amino acid residues, including Lys23/27/49/4, Asp27/Asp31, Trp25/29, Phe29/32, Cys26/30 to bind with *Torpedo* as well as *α7* receptor [31,32]. Along with Asp, Trp, Phe the amino acid Lysne and Cystine residues of the 3FTXs are essential for binding to nAChRs. It was also well established that Lysine and Cysteine have great affinity to bind with nanogold.

Lysine binds with the gold nanoparticles surface through it's ε-amine group (—NH_3+) with GNP surface whereas the binding of Cystein to GNP is mediated by covalent interaction through Thiol group (SH) associated with Cystine residues [33,34]. Therefore it may be assumed that the neurotoxicity of NKCT1 depends on the binding of its Lysine and Cystine residues to the nACh receptors and possibly GNP reduced the neurtoxicity of NKCT1 by altering its nACh specificity through binding to its Lysine or Cystine amino acid residues.

Previous research on 3FTXs reported that the myotoxic activity is a reflection of the myotoxic site of 3FTXs myotoxins, which contained a cationic segment flanking a hydrophobic region. Particularly the myotoxic region in cardiotoxins is located on all three loops with a row of positively charged Lysine residues [31]. This is a potent binding site for GNP, located at the top end of the NKCT1 and other 3FTXs. It was observed through CD spectra analysis of GNP-NKCT1 that GNP conjugation results in 20.5% increase in alpha helix, 5.5% increase in β-sheets and 32% of β-turn instead of random coil in NKCT1 [9]. The structural alteration of the NKCT1 after GNP conjugation may be responsible for the reduction of its toxicity profile. The exact molecular mechanism responsible for the reduction of the toxicity of NKCT1 is still not clear. Further studies on this area are warranted for the understanding of molecular mechanism related to the reduction of toxicity profile of the GNP-NKCT1 and its future applications.

5. Conclusion

It may be concluded that gold nanoparticle conjugation reduced the toxicity of snake venom protein toxin NKCT1. This work will definitely enlighten the opportunities of reducing toxicities of bioactive toxin molecules by nanoconjugation.

Conflict of interest

None declared.

Acknowledgement

This work was sponsored by Department of Biotechnology, Govt. of India, New Delhi, India (Ref. no. BT/PR14811/NNT/28/500/2010).

References

[1] A. Calmette, A. Saenz, L. Costil, Effets du venin de cobra sur les greffes cancereuses et sur le cancer spontane (adenocarcinoma) de la souris, C. R. Acad. Sci. 197 (1933) 205–210.
[2] A. Gomes, S. Bhattacharya, M. Chakraborty, P. Bhattacharjee, R. Mishra, Anti-arthritic activity of Indian monocellate cobra (*Naja kaouthia*) venom on adjuvant induced arthritis, Toxicon 55 (2010) 670–673.
[3] A. Debnath, A. Saha, A. Gomes, S. Biswas, P. Chakraborty, B. Giri, A.K. Biswas, S. Das Gupta, A. Gomes, A lethal cardiotoxic–cytotoxic protein from the Indian monocellate cobra (*Naja kaouthia*) venom, Toxicon 56 (2010) 569–579.
[4] A. Gomes, S. Royhoudhury, A. Saha, R. Mishra, B. Giri, A.K. Biswas, A. Debnath, A. Gomes, A heat stable protein toxin (drCT-I) from the Indian Viper (*Daboia russelli russelli*) venom having antiproliferative, cytotoxic and apoptotic activities, Toxicon 49 (1) (2007) 46–56.
[5] T. Das, S. Bhattacharya, B. Haldar, A. Biswas, S. Dasgupta, A. Gomes, A. Gomes, Cytotoxic and antioxidant property of a purified fraction (NN-32) of Indian *Naja naja* venom on Ehrlich ascites carcinoma in BALB/c mice, Toxicon 57 (2011) 1065–1072.
[6] J.E. Cura, D.P. Blanzaco, C. Brisson, Phase I and pharmacokinetics study of crotoxin (Cytotoxic PLA2, NSC-624244) in patients with advanced cancer, Clin. Cancer Res. 8 (2002) 1033–1041.
[7] L.A. Costa, H.A. Miles, R.A. Diez, C.E. Araujo, C.M. Coni Molina, J.C. Cervellino, Phase I study of VRCTC-310, a purified phospholipase A2 purified from snake venom, in patients with refractory cancer: safety and pharmacokinetic data, Anti-Cancer Drugs 8 (1997) 829–834.
[8] L.K. Kourounakis, R.A. Nelson, M.A. Kupusta, The effect of a cobra venom factor on complement and adjuvant induced disease in rats, Arthritis Rheum 16 (1) (1973) 71–76.
[9] T. Bhowmik, P.P. Saha, A. Dasgupta, A. Gomes, Antileukemic potential of PEGylated gold nanoparticle conjugated with protein toxin (NKCT1) isolated from Indian cobra (*Naja kaouthia*) venom, Cancer Nano 4 (1) (2013) 39–55.
[10] T.V. Freitas, F. Frézard, Encapsulation of native crotoxin in liposomes: a safe approach for the production of antivenom and vaccination against Crotalus durissus terrificus venom, Toxicon 35 (1) (1997) 91–100.
[11] H. Ernest, R. Shetty, Impact of nanotechnology on biomedical sciences: review of current concepts on convergence of nanotechnology with biology, Online J. Nanotechnol. 1 (2005) 1–14.
[12] M. Sivasankar, B.P. Kumar, Role of nanoparticles in drug delivery system, Int. J. Res. Pharm. Biomed. Sci. 1 (2) (2010) 41–66.
[13] A. Biswas, A. Gomes, J. Sengupta, P. Datta, S. Singha, A.K. Dasgupta, A. Gomes, Nanoparticle-conjugated animal venom-toxins and their possible therapeutic potential, J. Venom Res. 3 (2012) 15–21.
[14] N.R. Soman, S.L. Baldwin, G. Hu, J.N. Marsh, G.M. Lanza, J.E. Heuser, J.M. Arbeit, S.A. Wickline, P.H. Schlesinger, Molecularly targeted nanocarriers deliver the cytolytic peptide melittin specifically to tumor cells in mice, reducing tumor growth, J. Clin. Invest. 119 (2009) 2830–2842.
[15] N. Chanda, V. Kattumuri, R. Shukla, et al., Bombesin functionalized gold nanoparticles show in vitro and in vivo cancer receptor specificity, Proc. Natl. Acad. Sci. U.S.A. 107 (2010) 8760–8765.
[16] A. Debnath, Anticancer studies on the Indian snake venom (Doctoral dissertation), Jadavpur University, Calcutta, India, 2006.
[17] O.H. Lowry, N.J. Rosebrough, A.L. Farr, R.J. Randall, Protein measurement with the Folin phenol reagent, J. Biol. Chem. 193 (1951) 265–275.
[18] U.K. Laemmli, E. Molbert, M. Showe, Form-determining function of genes required for the assembly of the head of bacteriophage T4, E J. Mol. Biol. 49 (1970) 99–113.
[19] D. Lagunoff, E.P. Benditt, Mast cell degranulation and histamine release observed in a new in vitro system, J. Exp. Med. 112 (1960) 571–580.
[20] O. Langendorff, Untersuchungen am uberlebenden sangetierheazen, Pflugers Arch. Gas Physiol. 61 (1895) 291–332.
[21] J.H. Burn, Practical Pharmacology, Blackwell Scientific Publications, Oxford, 1952, pp. 22–25.
[22] M.H. Weisman, D.E. Furst, G.S. Park, J.M. Kremer, K.M. Smith, D.J. Wallace, J.R. Caldwell, T. Dervieux, Risk genotypes in folate-dependent enzymes and their association with methotrexate-related side effects in rheumatoid arthritis, Arthritis Rheum 54 (2) (2006) 607–612.
[23] A. Gomes, P. Datta, J. Sengupta, A. Biswas, A. Gomes, Evaluation of anti-arthritic property of methotrexate conjugated gold nanoparticle on experimental animal models, J. Nanopharm. Drug Deliv. 1 (2013) 206–211.
[24] S. Karmakar, D.C. Muhuri, S.C. Dasgupta, A.K. Nagchaudhuri, A. Gomes, Isolation of a haemorrhagic protein toxin (SA-HT) from the Indian venomous butterfish (*Scatophagus argus*, Linn.) sting extract, Indian J. Exp. Biol. 42 (5) (2004) 452–460.
[25] H.F. Chiu, I.J. Chen, C.M. Teng, Edema formation and degranulation of mast cells by a basic phospholipase A_2 purified from *Trimeresurus mucrosquamatus* snake venom, Toxicon 27 (1) (1989) 115–125.
[26] P.M. Guzy, Creatine phosphokinase-MB (CPK-MB) and the diagnosis of myocardial infarction, West J. Med. 127 (1977) 455–460.
[27] B.E. Sobel, W.E. Shell, Serum enzyme determinations in the diagnosis and assessment of myocardial infarction, Circulation 45 (1972) 471–482.
[28] J.C. Cutrin, B. Zingaro, S. Camandola, A. Boveris, A. Pompella, P. Giuseppe, Contribution of γ glutamyl transpeptidase to oxidative damage of ischemic rat kidney, Kidney Int. 57 (2000) 526–533.
[29] A.M. Safer, Ultrastructural localization of alkaline phosphatase activity in the proximal convoluted tubule cells of the gerbil *Meriones*

crassus using a cerium-based method, Eur. J. Histochem. 39 (2) (1995) 149–156.
[30] F. Danhier, E. Ansorena, J.M. Silva, R. Coco, A.L. Breton, V. Préat, PLGA-based nanoparticles: an overview of biomedical applications, J. Control. Release 161 (2012) 505–522.
[31] R.M. Kini, Molecular moulds with multiple missions: functional sites in three-finger toxins, Clin. Exp. Pharmacol. Physiol. 29 (2002) 815–822.
[32] A.V. Osipov, I.E. Kasheverov, Y.V. Makarova, V.G. Starkov, O.V. Vorontsova, R.K. Ziganshin, T.V. Andreeva, M.V. Merebryakova, A. Benoit, R.C. Hogg, D. Bertrand, V.I. Tsetlin, Y.N. Utkin, Naturally occurring disulfide-bound dimers of three-fingered toxins, J. Biol. Chem. 283 (2008) 14571–14580.
[33] R.K. DeLong, C.M. Reynolds, Y. Malcolm, A. Schaeffer, T. Severs, A. Wanekaya, Functionalized gold nanoparticles for the binding, stabilization, and delivery of therapeutic DNA, RNA, and other biological macromolecules, Nanotechnol. Sci. Appl. 33 (2010) 53–63.
[34] K. Siriwardana, A. Wang, Vangala k, N. Fitzkee, D. Zhang, Probing the effects of cysteine residues on protein adsorption onto gold nanoparticles using wild-type and mutated GB3 proteins, Langmuir 29 (35) (2013) 10990–10996.
[35] E. Bulbring, Observation on the isolated phrenic nerve diaphragm preparation of the rat, Br. J. Pharmacol. 1 (1952) 38–42.
[36] M.J. Sargent, G.C. Taylor, Appraisal of the MTT assay as a rapidtest of chemosensitivity in acute myeloid leukaemia, Br J Cancer 60 (1989) 206–210.